

## Articles

## Mechanism-Based Competitive Inhibitors of Glyoxalase I: Intracellular Delivery, in Vitro Antitumor Activities, and Stabilities in Human Serum and Mouse Serum

Malcolm J. Kavarana,<sup>†</sup> Elena G. Kovaleva,<sup>†</sup> Donald J. Creighton,<sup>\*,†</sup> Megan B. Wollman,<sup>‡</sup> and Julie L. Eiseman<sup>\*,‡,§</sup>

Department of Chemistry and Biochemistry, University of Maryland Baltimore County, Baltimore, Maryland 21250, and Division of Developmental Therapeutics, Greenebaum Cancer Center, and Department of Pathology, University of Maryland, Baltimore, Baltimore, Maryland 21201

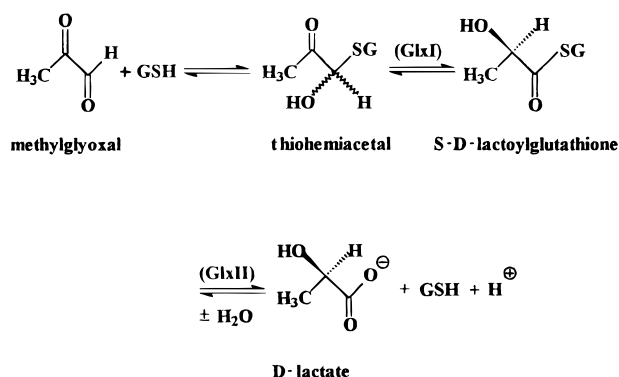
Received October 21, 1998

*S*-(*N*-Aryl-*N*-hydroxycarbamoyl)glutathione derivatives (GSC(O)N(OH)C<sub>6</sub>H<sub>4</sub>X, where GS = glutathionyl and X = H (**1**), Cl (**2**), Br (**3**)) have been proposed as possible anticancer agents, because of their ability to strongly inhibit the methylglyoxal-detoxifying enzyme glyoxalase I. In order to test this hypothesis, the in vitro antitumor activities of these compounds and their [glycyl,glutamy] diethyl ester prodrug forms (**1**(Et)<sub>2</sub>–**3**(Et)<sub>2</sub>) have been examined. All three diethyl esters inhibit the growth of L1210 murine leukemia and B16 melanotic melanoma in culture, with GI<sub>50</sub> values in the micromolar concentration range. Cell permeability studies with L1210 cells indicate that growth inhibition is associated with rapid diffusion of the diethyl esters into the cells, followed by enzymatic hydrolysis of the ethyl ester functions to give the inhibitory diacids. In contrast, the corresponding diacids neither readily diffuse into nor significantly inhibit the growth of these cells. Consistent with the hypothesis that cell growth inhibition is due to competitive inhibition of glyoxalase I, preincubation of L1210 cells with **2**(Et)<sub>2</sub> increases the sensitivity of these cells to the inhibitory effects of exogenous methylglyoxal. Compound **2**(Et)<sub>2</sub> is much less toxic to nonproliferating murine splenic lymphocytes, possibly reflecting reduced sensitivity to methylglyoxal and/or reduced chemical stability of the diacid inside these cells. Finally, a plasma esterase-deficient murine model has been identified that should allow in vivo testing of the diethyl esters.

### Introduction

Progress in understanding methylglyoxal metabolism in mammalian cells suggests that the glyoxalase enzyme system might be a reasonable target for antitumor drug development.<sup>1</sup> The apparent physiological function of this pathway is to remove cytotoxic methylglyoxal from cells as D-lactate via the sequential action of the isomerase glyoxalase I (GlxI) and the thioester hydrolase glyoxalase II (GlxII), Scheme 1. Methylglyoxal appears to arise primarily as a byproduct of the interconversion of intracellular triosephosphates, as well as from other sources.<sup>3,4</sup> High concentrations of exogenous methylglyoxal selectively inhibit rapidly dividing tumor cells versus quiescent normal cells in vitro.<sup>5–8</sup> The molecular basis of this activity is not clearly understood but probably involves inhibition of DNA and protein synthesis.<sup>5,9</sup> Indeed, methylglyoxal is known to form adducts with nucleic acids.<sup>10</sup> Several observations support a detoxification role for the glyoxalase pathway. Among these is the recent demonstration that transfected murine NIH3T3 cells that overexpress the gene

Scheme 1. Glyoxalase Enzyme System<sup>a</sup>



<sup>a</sup> Symbols: GSH, glutathione ( $\gamma$ -L-Glu-L-CysGly); GlxI, glyoxalase I (EC 4.4.1.5); GlxII, glyoxalase II (EC 3.1.2.6) (for reviews, see refs 2 and 3).

for GlxI are exceptionally resistant to the cytotoxic effects of exogenous methylglyoxal.<sup>11</sup>

Vince and Daluge were the first to suggest that inhibitors of GlxI might function as antitumor agents by inducing elevated levels of methylglyoxal in cells.<sup>12</sup> Although numerous GSH-based competitive inhibitors have been described in the literature, a method for efficiently delivering these compounds into cells has not

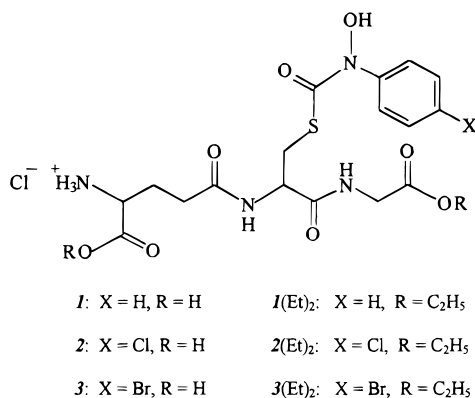
\* Corresponding authors. Tel: (410) 455-2491 (D.J.C.); (410) 455-2518 (J.L.E.). Fax: (410) 455-2608.

<sup>†</sup> Department of Chemistry and Biochemistry.

<sup>‡</sup> Greenebaum Cancer Center.

<sup>§</sup> Department of Pathology.

**Chart 1.** *S*-(*N*-Aryl-*N*-hydroxycarbamoyl)glutathione Derivatives (R = H) and Their [*Glycyl, Glutamyl*] Diethyl Esters (R = C<sub>2</sub>H<sub>5</sub>)



been available. Importantly, Lo and Thornalley recently reported that the competitive inhibitor *S*-(*p*-bromobenzyl)glutathione can be indirectly delivered into HL60 human leukemia cells as the [*glycyl, glutamyl*] diethyl ester prodrug, as intracellular esterases catalyze the deesterification of the diester to give the inhibitory diacid.<sup>13</sup> Moreover, the diester was reported to be toxic to these cells. The same laboratory subsequently found that the cyclopentyl diester prodrug form of this compound inhibits the growth of several different human tumors *in vitro*<sup>14</sup> and a murine adenocarcinoma *in vivo*.<sup>15</sup> These effects were tentatively attributed to inhibition of GlxI.

As part of a research program aimed at developing mechanism-based competitive inhibitors of GlxI, we recently demonstrated that the *N*-aryl-*N*-hydroxycarbamoyl esters of GSH (**1–3**), shown in Chart 1, are the strongest competitive inhibitors of this enzyme yet reported, with *K*<sub>i</sub> values in the nanomolar concentration range.<sup>16,17</sup> Tight binding appears to reflect their stereo-electronic similarity to the tightly bound enediol intermediate that forms along the reaction coordinate of GlxI and the presence of a hydrophobic binding pocket in the active site. In principle, the diethyl esters of the enediol analogues might prove to be potent inhibitors of tumor growth, given their high affinity for GlxI. In addition, they might also be selective tumoricidal agents, because quiescent cells often contain much higher levels of GlxII activity than cancer cells.<sup>18,19</sup> Since GlxII catalyzes the slow hydrolytic decarbamoylation of the enediol analogues, the enediol analogues might be less stable in normal cells than in cancer cells and, therefore, less toxic to normal cells.<sup>17</sup>

In this report, we show that prodrugs **1**(Et)<sub>2</sub>–**3**(Et)<sub>2</sub> selectively inhibit the growth of L1210 murine leukemia and B16 melanotic melanoma versus quiescent splenic lymphocytes. Evidence is presented that growth inhibition of the tumor cell lines probably arises from inhibition of the glyoxalase pathway, although the basis of selective toxicity is unclear. During the course of these studies, the prodrugs were found to undergo rapid deesterification in serum from inbred strains of laboratory mice, but only slow deesterification in human serum. This might preclude efficacy studies in mice, because the prodrug would be inactivated before reaching the target tumor. Importantly, we have identified a strain of plasma esterase-deficient tumor-bearing mice

**Table 1.** In Vivo Inhibition of L1210 Leukemia and B16 Melanoma by Different Competitive Inhibitors of GlxI (RPMI 1640/10% fetal calf serum, 37 °C, 48 h)

inhibitor	<i>K</i> <sub>i</sub> (μM) <sup>a</sup>	GI <sub>50</sub> (μM) <sup>b</sup>	TGI (μM) <sup>c</sup>	LC <sub>50</sub> (μM) <sup>d</sup>	<i>n</i> <sup>e</sup>
L1210 Cells					
<b>1</b> (Et) <sub>2</sub>	0.16	84 ± 47	135 ± 5	271 ± 5	3
<b>2</b> (Et) <sub>2</sub>	0.046	7 ± 3	27 ± 10	54 ± 5	3
<b>3</b> (Et) <sub>2</sub>	0.014	3 ± 2	7 ± 3	17 ± 7	3
<i>p</i> -BrBzSG(Et) <sub>2</sub> <sup>f</sup>	0.17	7 ± 2	11 ± 2	26 ± 3	3
B16 Cells					
<b>1</b> (Et) <sub>2</sub>	0.16	>100	>100	>100	1
<b>2</b> (Et) <sub>2</sub>	0.046	15 ± 3	~23 <sup>g</sup>	~47 <sup>g</sup>	3
<b>3</b> (Et) <sub>2</sub>	0.014	11 ± 4	33 ± 2	54 ± 1	3
<i>p</i> -BrBzSG(Et) <sub>2</sub> <sup>f</sup>	0.17	14 ± 4	~23 <sup>g</sup>	~56 <sup>g</sup>	3

<sup>a</sup> Competitive inhibition constants of the unesterified species with human erythrocyte GlxI.<sup>17</sup> <sup>b</sup> GI<sub>50</sub>, concentration producing 50% growth inhibition in comparison to no-drug controls. <sup>c</sup> TGI, concentration producing 100% growth inhibition. <sup>d</sup> LC<sub>50</sub>, concentration producing 50% cell killing. <sup>e</sup> Number of different experiments from which the mean and standard deviation are calculated. <sup>f</sup> *S*-(*p*-Bromobenzyl)glutathione diethyl ester. <sup>g</sup> Interpolated value from one experiment.

that model the low esterase activity in human serum, opening the way for *in vivo* efficacy studies of the enediol analogue diethyl esters.

## Chemistry

The *S*-(*N*-aryl-*N*-hydroxycarbamoyl)glutathione derivatives **1–3** were prepared by the reaction of GSH and the 4-chlorophenyl esters of the corresponding *N*-hydroxycarbamates, as previously described.<sup>17</sup> *S*-(*p*-Bromobenzyl)glutathione was prepared by the method of Vince et al.<sup>20</sup> The diethyl esters of these compounds were obtained by acid-catalyzed esterification of the diacids in ethanolic HCl. The diester preparations were then purified to greater than 98% homogeneity by reverse-phase C<sub>18</sub> HPLC. The analytical data on *S*-(*p*-bromobenzyl)glutathione diethyl ester are identical to the literature values.<sup>13</sup>

## Results

**Cytotoxicity Studies.** In order to assess the enediol analogue diethyl esters **1**(Et)<sub>2</sub>–**3**(Et)<sub>2</sub> as tumor-selective anticancer agents, they were evaluated against B16 melanotic melanoma, L1210 murine leukemia, and nonproliferating murine splenic lymphocytes in culture. *S*-(*p*-Bromobenzyl)glutathione diethyl ester was used as a positive control. These compounds were found to be cytostatic and cytotoxic to both tumor cell lines, Table 1. The growth inhibition parameters GI<sub>50</sub> and TGI, corresponding to 50% and total growth inhibition (respectively), and the cytotoxicity parameter LC<sub>50</sub>, corresponding to 50% cell killing, were obtained as interpolated values from the dose–response curves, e.g., Figure 1. Percentage growth was calculated by a method analogous to that used by the U.S. National Cancer Institute in their human tumor screening program.<sup>22</sup> The dose–response data were obtained under conditions where fresh diethyl ester was added to the tissue culture medium at 0, 12, 24, and 36 h. This was intended to partially compensate for spontaneous deesterification of the diethyl esters in the culture medium (*t*<sub>1/2</sub> = 2.5 ± 0.5 h), monitored by reverse-phase C<sub>18</sub> HPLC.

The relative potencies of **1**(Et)<sub>2</sub>–**3**(Et)<sub>2</sub> might be explained by competitive inhibition of GlxI by intracellular enediol analogue. The values of the cell inhibition

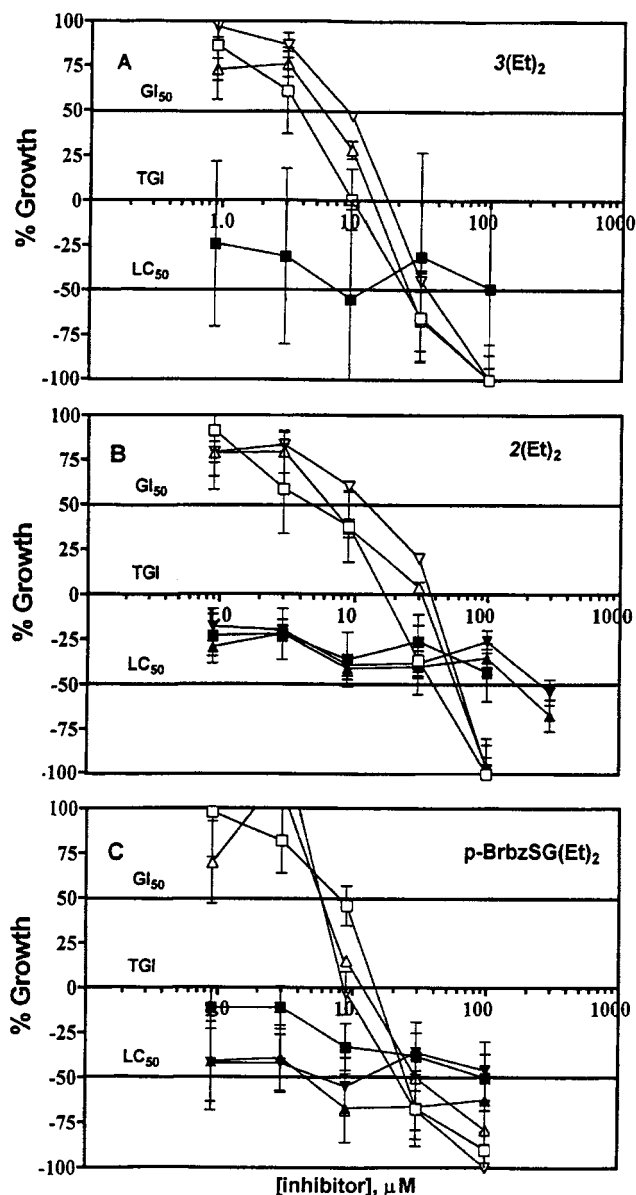


**Figure 1.** Growth inhibition of L1210 cells (open symbols) and splenic lymphocytes (closed symbols) by (A) *S*-(*N*-(*p*-bromophenyl)-*N*-hydroxycarbonyl)glutathione diethyl ester (**3**(Et)<sub>2</sub>), (B) *S*-(*N*-(*p*-chlorophenyl)-*N*-hydroxycarbonyl)glutathione diethyl ester (**2**(Et)<sub>2</sub>), and (C) *S*-(*p*-bromobenzyl)glutathione diethyl ester (*p*-BrbzSG(Et)<sub>2</sub>) (RPMI 1640/10% fetal calf serum, 37 °C, 48 h). For L1210 cells, percentage growth (PG) was calculated from the following relationships: When  $(\rho_{\text{test}} - \rho_{\text{tzero}}) \geq 0$ ,  $\text{PG} = 100 \times (\rho_{\text{test}} - \rho_{\text{tzero}}) / (\rho_{\text{ctrl}} - \rho_{\text{tzero}})$ , where  $\rho_{\text{tzero}}$  is cell density prior to exposure to drug,  $\rho_{\text{test}}$  is cell density after a 48-h exposure to the drug, and  $\rho_{\text{ctrl}}$  is cell density after 48 h with no exposure to the drug. When  $(\rho_{\text{test}} - \rho_{\text{tzero}}) < 0$ ,  $\text{PG} = 100 \times (\rho_{\text{test}} - \rho_{\text{tzero}}) / \rho_{\text{tzero}}$ . For splenic lymphocytes, PG was calculated from the relationship:  $\text{PG} = 100 \times (\rho_{\text{test}} - \rho_{\text{ctrl}}) / \rho_{\text{ctrl}}$ . Different symbols correspond to experiments carried out on different days. Error bars represent standard deviations for triplicate determinations.

constants for both tumor cell lines decrease with decreasing values of the competitive inhibition constants ( $K_i$ 's) of **1–3** with human erythrocyte GlxI, Table 1. In the case of L1210 cells, the 11-fold difference in  $K_i$  values for **1** versus **3** is associated with an approximate 28-fold difference in the  $\text{GI}_{50}$  values for **1**(Et)<sub>2</sub> versus **3**(Et)<sub>2</sub>. On the other hand, the structurally different *S*-(*p*-bromobenzyl)glutathione diethyl ester does not fit the

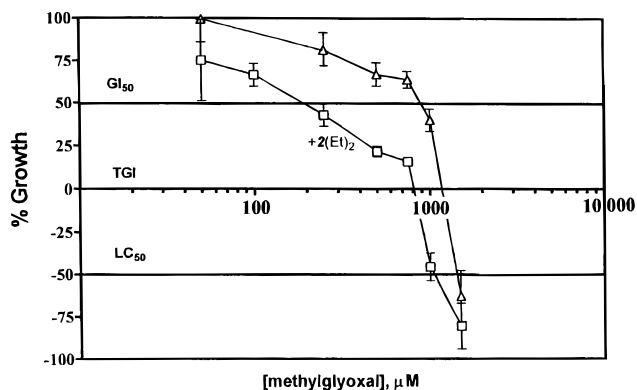


**Figure 2.** Growth inhibition of L1210 cells by methylglyoxal (triangles) and methylglyoxal after preincubation of the cells for 2 h in the presence of **2**(Et)<sub>2</sub> at its  $\text{GI}_{50}$  concentration (squares) (RPMI 1640/10% fetal calf serum, 37 °C, 48 h). Percentage growth was calculated as described in the legend to Figure 1. These experiments were run in parallel on the same day.

correlation observed with the enediol analogue diethyl esters. For example, enediol analogue **1** and *S*-(*p*-bromobenzyl)glutathione have nearly identical  $K_i$  values, but the  $\text{GI}_{50}$  value for **1**(Et)<sub>2</sub> is roughly 10-fold larger than that for *S*-(*p*-bromobenzyl)glutathione diethyl ester with each tumor cell line. Thus, the structure–activity relationships are ambiguous with respect to the mechanism of cell inhibition by structurally different compounds. A more direct test of the hypothesis that potency is due to inhibition of GlxI involved determining whether preincubation of L1210 cells with **2**(Et)<sub>2</sub> increases the sensitivity of the cells to the inhibitory properties of exogenous methylglyoxal. Indeed, preincubation of these cells for 2 h with **2**(Et)<sub>2</sub> at its  $\text{GI}_{50}$  concentration caused an approximate 5-fold decrease in the  $\text{GI}_{50}$  concentration of methylglyoxal with these cells, Figure 2.

With respect to tumor selectivity, the diethyl esters **2**(Et)<sub>2</sub> and **3**(Et)<sub>2</sub> are relatively poor inhibitors of murine splenic lymphocytes, Figure 1. Concentrations of the diethyl esters (100  $\mu\text{M}$ ) producing nearly 100% killing of L1210 cells caused a decrease in the viability of splenic lymphocytes by less than 50%. This effect could be due, in part, to the reduced ability of L1210 cells to catalyze the decarbonylation of intracellular enediol analogue. The GlxII activities in the L1210 cells ( $0.02 \pm 0.003$  U/mg of protein) used in this study were about 10-fold lower than that in splenic lymphocytes ( $0.20 \pm 0.03$  U/mg of protein). In contrast, the GlxI activities in the L1210 cells ( $0.31 \pm 0.03$  U/mg of protein) were about equal to that in splenic lymphocytes ( $0.36 \pm 0.03$  U/mg of protein). However, *S*-(*p*-bromobenzyl)glutathione diethyl ester also shows selective inhibitory activity toward L1210 cells versus splenic lymphocytes, Figure 1. This compound cannot undergo hydrolytic decomposition in the presence of GlxII and, therefore, provides a control for toxic effects resulting exclusively from inhibition of GlxI. Thus, the differential toxicities observed with the enediol analogue diethyl esters might reflect differences in GlxII activity between L1210 cells and splenic lymphocytes and/or differences in the intrinsic susceptibilities of each cell line to the toxic effects of methylglyoxal. Conceivably, selective toxicity might arise as an artifact due to the presence of membrane-



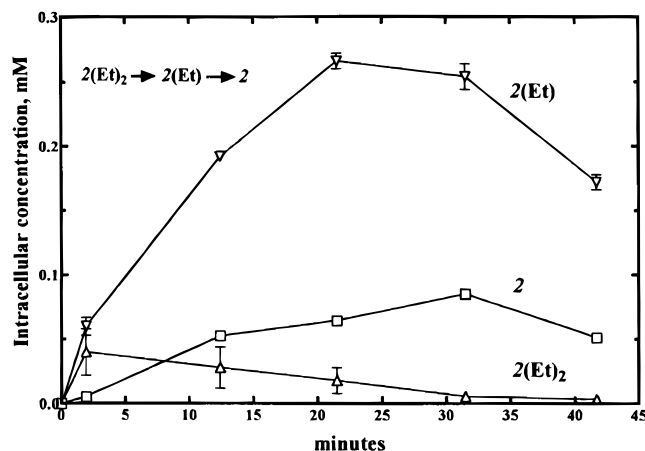


**Figure 3.** Time-dependent change in the intracellular concentration of *S*-(*N*-(*p*-chlorophenyl)-*N*-hydroxycarbonyl)glutathione (**2**) (squares), the [glycyl] monoethyl ester (**2**(Et)) (inverted triangles), and the diethyl ester (**2**(Et)<sub>2</sub>) (triangles) in L1210 cells incubated in the presence of 0.1 mM **2**(Et)<sub>2</sub> (RPMI 1640/10% fetal calf serum, 37 °C). Error bars represent standard deviations for triplicate determinations.

bound esterases on the surfaces of splenic lymphocytes and L1210 cells. Since the initial cell densities for the toxicity studies with lymphocytes were about 25-fold larger than that with the L1210 cells, this would result in more rapid deesterification of the extracellular enediol esters (and lower apparent toxicity) with the lymphocytes. However, this explanation seems less likely, on the basis of our observation that the sensitivity of splenic lymphocytes to *S*-(*p*-bromobenzyl)glutathione diethyl ester is about the same, whether the initial cell density is  $\sim 10^6$  or  $\sim 10^7$  cells/mL.

**Cell Permeability Studies.** The potencies of the enediol analogue diethyl esters presumably reflect rapid diffusion of the diesters across the cell membrane, followed by catalytic deesterification to give the inhibitory diacid form of the enediol analogue. Indeed, the diacids alone do not readily diffuse into cells. Incubation of L1210 cells with 0.15 mM **2** for a period of 225 min showed no time-dependent increase in the concentration of **2** in the intracellular fraction, monitored by reverse-phase C<sub>18</sub> HPLC. Moreover, all of the enediol analogues **1–3** were much less toxic to L1210 and B16 cells than the corresponding diesters (data not shown). In contrast, incubation of L1210 cells with 0.1 mM **2**(Et)<sub>2</sub> showed the appearance of three major species in the intracellular fraction that comigrated with authentic samples of **2**(Et)<sub>2</sub>, **2**[glycyl](Et), and **2** on a reverse-phase column, Figure 3. Transport was characterized by a rapid initial increase in the concentrations of the mono- and diethyl esters, followed by a slower increase in the concentration of the diacid **2**. This is consistent with a model in which intracellular **2** arises from the sequential deethylation of intracellular **2**(Et)<sub>2</sub>. The decreasing concentrations of all three species at longer times could be due to a combination of effects including hydrolytic deethylation of extracellular **2**(Et)<sub>2</sub> and GlxII-catalyzed decarbonylation of intracellular **2**. Consistent with simple passive diffusion of **2**(Et)<sub>2</sub> across the cell membrane, the initial rates of appearance of the sum of all of the intracellular species were a linear function of extracellular [**2**(Et)<sub>2</sub>] in the range 0.05–0.5 mM; i.e., there was no evidence for saturation kinetics, Figure 4. Also

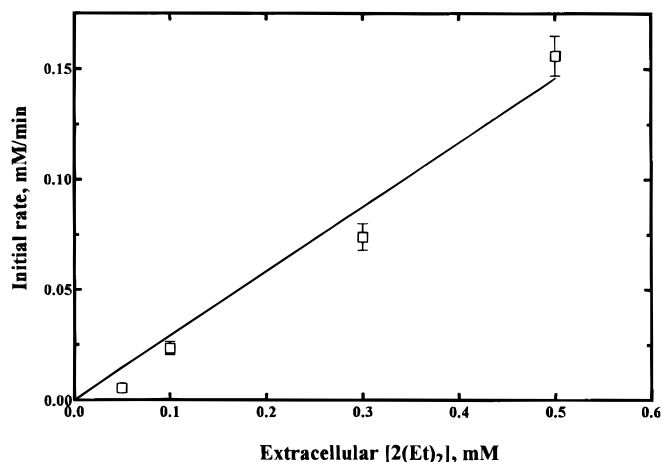


**Figure 4.** Initial rates of appearance of the sum of *S*-(*N*-(*p*-chlorophenyl)-*N*-hydroxycarbonyl)glutathione (**2**), the [glycyl] monoethyl ester (**2**(Et)), and the diethyl ester (**2**(Et)<sub>2</sub>) in L1210 cells as a function of extracellular [**2**(Et)<sub>2</sub>] (RPMI 1640/10% fetal calf serum, 37 °C). Error bars represent standard deviations for triplicate determinations.

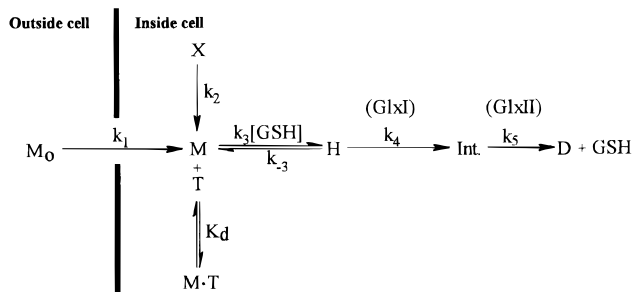
consistent with this model, the *n*-octanol/water partition coefficient of **2**(Et)<sub>2</sub> ( $p = 93 \pm 5$ ) is at least ( $9 \times 10^3$ )-fold larger than that of **2** ( $p < 0.01$ ).

**Stability of **2**(Et)<sub>2</sub> in Human Serum and Mouse Serum.** In principle, the enediol analogue diesters might be used to treat human tumors provided that the diesters are reasonably stable in human serum. Indeed, **2**(Et)<sub>2</sub> undergoes only slow deesterification in serum samples obtained from four different individuals ( $t_{1/2} = 9.1 \pm 5.3$  h ( $n = 4$ )), monitored by reverse-phase C<sub>18</sub> HPLC. Unfortunately, **2**(Et)<sub>2</sub> undergoes extremely rapid deesterification ( $t_{1/2} < 30$  s) in serum samples obtained from inbred strains of laboratory mice used to evaluate chemotherapeutic agents against murine tumors and human tumor xenografts: DBA/2, C57BL/6, NCr nu/nu, and CD<sub>2</sub>F<sub>1</sub>. Presumably, this would lead to inactivation of the prodrug before it reached the target tumor. This prompted an evaluation of the stability of **2**(Et)<sub>2</sub> in serum samples obtained from plasma esterase-deficient DBA/2 × C57BL/6 mice, supplied by Jackson Laboratories. Importantly, the stability of **2**(Et)<sub>2</sub> was found to be similar to that in human serum:  $t_{1/2} = 3.9 \pm 0.6$  h ( $n = 5$ ).

## Discussion

The central observation of this work is that the diethyl esters of the enediol analogues shown in Chart 1 are both cytostatic and cytotoxic to murine leukemia L1210 and B16 melanotic melanoma cells in culture (Table 1) but are much less toxic to nonproliferating splenic lymphocytes (Figure 1). This is the first demonstration that mechanism-based competitive inhibitors of GlxI are potentially important antitumor agents. Several observations suggest that inhibition of intracellular GlxI plays an important role in inhibiting tumor growth, as discussed below.

**Cell Permeability Studies.** Cell growth inhibition is associated with the intracellular delivery of the enediol analogues as their diethyl esters, a strategy that depends upon the presence of intracellular esterases to remove the ethyl functions. This prodrug strategy has previously been used to deliver *S*-(*p*-bromobenzyl)-

**Scheme 2.** Kinetic Model of the Glyoxalase Pathway Inside a Tumor Cell

Where M = methylglyoxal

X = chemical species giving rise to methylglyoxal

T = target(s) to which methylglyoxal binds in order to inhibit cells

H = thiohemiacetal

Int. = S-D-lactoylglutathione

D = D-lactate

glutathione into human leukemia (HL60) cells.<sup>14</sup> Several factors might influence the steady-state concentration of the enediol analogues inside cells, including the rate of passive diffusion of the diester across the cell membrane, the rate of enzyme-catalyzed deesterification of the diester to give the enediol analogue, and GlxII-catalyzed decarbamoylation of the enediol analogue. Evidence has also been presented for the presence of an ATP-dependent GSH conjugate "export pump" in different tumor cell lines,<sup>22</sup> including L1210 cells,<sup>23</sup> which could remove enediol analogue from tumor cells. Nevertheless, under the conditions of the cell permeability studies, the pump is not able to decrease the steady-state concentration of the enediol analogue to nontoxic levels. Finally, the potencies of GlxI inhibitors in general might be influenced by the chemical nature of the diester substituents. Thornalley and co-workers report that the dicyclopentyl ester of *S*-(*p*-bromobenzyl)-glutathione is twice as potent as the diethyl ester to HL60 cells in culture.<sup>14</sup> This might reflect more rapid diffusion of the dicyclopentyl ester into the cells and/or more rapid deesterification by intracellular esterases.

**Cytotoxicity Studies.** The inhibitory properties of the extracellular enediol analogue diethyl esters can be reasonably explained by binding of intracellular enediol analogue to the active site of GlxI, causing the buildup of cytotoxic methylglyoxal. This hypothesis is strengthened by the fact that L1210 cells exhibit enhanced sensitivity to extracellular methylglyoxal when the cells are preloaded with enediol analogue. It is instructive to interpret these effects in terms of the minimum kinetic model shown in Scheme 2, in which the glyoxalase pathway is assumed to be the only means of removing methylglyoxal from cells. In scheme 2, each enzyme-catalyzed step is reasonably depicted as being essentially irreversible, as discussed elsewhere.<sup>24</sup> Intracellular methylglyoxal, in its unhydrated form, is shown to arise either as a byproduct of normal intermediary metabolism ( $k_2(X)$ ) or from diffusion of exogenous methylglyoxal hydrates into the cell, followed by dehydration to give unhydrated methylglyoxal ( $k_1(M_0)$ ). Cell growth inhibition is postulated to reflect equilibrium binding of unhydrated methylglyoxal to one or

more target sites within the cell. The following analysis allows a tentative assessment of the relationship between the binding affinities of the enediol analogues for GlxI and tumor toxicity.

The GlxI reaction appears to be significantly rate-limiting in some types of tumor cells. The sensitivity of tumor cells to inhibitors of GlxI will depend, in part, on the extent to which the GlxI reaction limits the overall velocity of the glyoxalase pathway. In a previous study, we concluded that the GlxI reaction in mammalian erythrocytes is about 50% rate-determining overall, on the basis of the near equality of the measured values of  $k_{cat}[E_t]/K_m$  for the GlxI reaction ( $k_4$ ) and the rate constant for conversion of GSH-methylglyoxal thiohemiacetal substrates back to free GSH and unhydrated methylglyoxal at pH 7 ( $k_{-3}$ ).<sup>24,25</sup> The GlxI reaction also appears to be about 50% rate-limiting in NIH3T3 cells, given that the  $IC_{50}$  ( $\sim GI_{50}$ ) value of methylglyoxal with these cells increases by about 2-fold when the cells are transfected with the gene for GlxI overexpressing GlxI activity by 10-fold in comparison to wild-type cells.<sup>11</sup> This conclusion is based on the following reasoning:

Assuming that the binding equilibrium between M and T, shown in Scheme 2, is a slow process in comparison to the rates of formation and loss of methylglyoxal, the *net* rate of formation of intracellular methylglyoxal is given by:

$$d[M]/dt = k_1[M_0] + k_2[X] - ((k_3k_4)/(k_{-3} + k_4))[GSH]_t [M] \quad (1)$$

This equation applies under subsaturating conditions, where  $k_4$  is equal to  $k_{cat}[E_t]/K_m$  for GlxI. Therefore, under steady-state conditions ( $d[M]/dt \approx 0$ ):

$$[M]_{ss} \approx (k_1[M_0] + k_2[X])/((k_3k_4)/(k_{-3} + k_4))[GSH]_t \quad (2)$$

The fraction  $F$  of target sites occupied by methylglyoxal (MT) is given by:

$$F \approx \{1 + K_d\{((k_3k_4)/(k_{-3} + k_4))[GSH]/(k_1[M_0] + k_2[X])\}\}^{-1} \quad (3)$$

obtained by combining eq 2 with  $K_d = [M_{ss}][T]/[MT]$  and  $F = [MT]/([MT] + [T])$ .

In the special case where intracellular methylglyoxal is being generated primarily from methylglyoxal in the growth medium ( $k_1[M_0] \gg k_2[X]$ ), eq 3 reduces to eq 4:

$$F \approx \{1 + K_d\{((k_3k_4)/(k_{-3} + k_4))[GSH]/k_1[M_0]\}\}^{-1} \quad (4)$$

This equation can be related to the  $GI_{50}$  of methylglyoxal, assuming that the rate of cell growth is inversely proportional to  $F$  and that  $M_0 = GI_{50}$  when  $F = 0.5$ :

$$GI_{50} \approx (K_d/k_1)\{k_3k_4/(k_{-3} + k_4)\}[GSH] \quad (5)$$

This equation indicates that the  $GI_{50}$  would increase by 2-fold when  $k_4$  increases by 10-fold, only when  $k_{-3} \approx k_4$  in wild-type cells; i.e., when the GlxI reaction is about 50% rate-limiting in wild-type cells. This implies that the GlxI reaction might be significantly rate-determining in tumor cells in general.

The GlxI reaction in L1210 cells is significantly inhibited in the presence of enediol analogue diethyl ester

**2(Et)<sub>2</sub>**. The observation that the GI<sub>50</sub> of methylglyoxal with L1210 cells decreases by a factor of about 5 after preincubation of the cells with **2(Et)<sub>2</sub>** suggests that intracellular enediol analogue **2** inhibits GlxI. The extent of inhibition depends upon the degree to which the GlxI reaction is rate-limiting, the magnitude of the dissociation constant of the enediol analogue for the active site of GlxI (*K<sub>i</sub>*), and the accessibility of the enediol analogue to the enzyme. This is quantitatively expressed in eq 6:

$$GI_{50} \approx (K_d/k_1)\{k_3/(1 + (k_{-3}/k_4))(1 + [I_1]/K_i)\}[GSH] \quad (6)$$

obtained by combining eq 5 with the equation for competitive enzyme inhibition. In the equation, I<sub>1</sub> is intracellular enediol analogue available to inhibit GlxI. Assuming that the GlxI reaction is about 50% rate-limiting in L1210 cells (*k<sub>-3</sub>* ≈ *k<sub>4</sub>*), the 5-fold decrease in the GI<sub>50</sub> of methylglyoxal in cells preloaded with enediol analogue **2** suggests that the average extent of inhibition of GlxI is greater than 90% over the course of the inhibition study (i.e., [I]/*K<sub>i</sub>* ≈ 8).

The kinetic model of Scheme 2 also predicts that the GI<sub>50</sub> values of the GlxI inhibitors with L1210 and B16 melanotic melanoma cells should parallel the *K<sub>i</sub>* values of the corresponding diacids with human GlxI (Table 1). However, *S*-(*p*-bromobenzyl)glutathione diethyl ester does not follow the trend observed with the enediol analogue diethyl esters, as previously emphasized. This might indicate that growth inhibition arises from effects other than just competitive inhibition of GlxI. Alternatively, the steady-state concentration of *S*-(*p*-bromobenzyl)glutathione inside the tumor cells might be significantly higher than that of the enediol analogues, because *S*-(*p*-bromobenzyl)glutathione is not a substrate for GlxII. Additional experiments are needed in order to resolve this ambiguity.

In principle, growth inhibition might also arise from competitive inhibition of GlxII. We previously demonstrated that the enediol analogues function as apparent competitive inhibitors of bovine liver GlxII, as these compounds are only slowly hydrolyzed by the enzyme.<sup>17</sup> Thus, inhibition of GlxII would give rise to elevated steady-state levels of *S*-D-lactoylglutathione inside cells. Indeed, evidence has been presented that this metabolite inhibits the growth of HL60 cells in culture.<sup>26</sup> Principato and co-workers recently demonstrated that *S*-(fluorenylmethoxycarbonyl)glutathione diisopropyl ester inhibits the growth of rat adrenal pheochromocytoma PC-12 cells in culture with an IC<sub>50</sub> of 275 μM.<sup>27</sup> This might be due to the accumulation of *S*-D-lactoylglutathione, as the *K<sub>i</sub>* value of *S*-(fluorenylmethoxycarbonyl)glutathione obtained with a PC-12 cell extract of GlxII is about 3-fold smaller than that obtained with a PC-12 cell extract of GlxI. However, this explanation seems less likely in our case, because the *K<sub>i</sub>* values of the enediol analogues with GlxII are approximately 100-fold larger than those with GlxI.<sup>17</sup> This would preclude the accumulation of *S*-D-lactoylglutathione, assuming that both enzymes are equally accessible to the inhibitor inside the cells.

Having established the toxicities of the enediol analogue diethyl ester toward murine tumors in vitro and a plausible kinetic model to explain these effects, the next step will be to evaluate the in vivo efficacies of

these compounds. The plasma esterase-deficient DBA/2×C57BL/6 mice supplied by Jackson Laboratories appear to be an appropriate murine model for in vivo testing. These mice were developed from an inbred strain of tumor-bearing mouse, DBA/2J, carrying a new allele of the esterase locus (*Es-1*), designated *Es-1<sup>e</sup>*.<sup>28</sup> Zymogram patterns show that the ES-1E esterase migrates to a position between those of ES-1A and ES-1B and has much less enzyme activity. Moreover, the mutation is heritable, and there is no apparent detrimental effect to the mutant-bearing animals. These mice are an important advance on the way toward ultimately evaluating the clinical properties of these mechanism-based competitive inhibitors of GlxI, as well as other antitumor drugs containing critical ester functions.

## Experimental Section

NMR spectra were taken on a GE QE-300 NMR spectrometer. Mass spectral data were obtained at the Midwest Center for Mass Spectrometry, University of Nebraska—Lincoln. Elemental analyses were obtained at Atlantic Microlabs, Inc., Norcross, GA.

***S*-(*N*-Aryl-*N*-hydroxycarbamoyl)glutathiones 1–3 and the Diethyl Esters 1(Et)<sub>2</sub>–3(Et)<sub>2</sub>**. The diacids **1–3** were prepared by acyl-interchange reactions between excess GSH and the 4-chlorophenyl esters of the corresponding *N*-aryl-*N*-hydroxycarbamates, as previously described.<sup>17</sup> The diethyl esters **1(Et)<sub>2</sub>–3(Et)<sub>2</sub>** were prepared by acid-catalyzed esterification of **1–3** in ethanolic HCl (1.9 N) (~25 h, room temperature). Removal of the solvent in vacuo gave the hydrochloride salt of the diethyl ester in greater than 90% yield. The diethyl esters could be purified from trace amounts of monoethyl ester by reverse-phase C-18 column chromatography using methanol/water (1:1) containing 0.25% acetic acid as an eluting solvent. Removal of the solvent from the peak fractions gave the acetate salt of the diethyl ester. For **1(Et)<sub>2</sub>** (HCl salt): 300 MHz <sup>1</sup>H NMR (D<sub>2</sub>O, DSS) δ 1.25 (6H, m, ethyl-CH<sub>3</sub>), 2.21 (2H, m, Glu-C<sub>β</sub>H<sub>2</sub>), 2.56 (2H, m, Glu-C<sub>γ</sub>H<sub>2</sub>), 3.20 (1H, q, Cys-C<sub>β</sub>H<sub>a</sub>, *J* = 7.8, 14.5 Hz), 3.42 (1H, q, Cys-C<sub>β</sub>H<sub>b</sub>, *J* = 5.1, 14.5 Hz), 4.01 (2H, s, Gly-CH<sub>2</sub>), 4.1 (1H, t, Glu-C<sub>α</sub>H, *J* = 6.0 Hz), 4.23 (4H, m, ethyl-CH<sub>2</sub>), 4.67 (1H, m, Cys-C<sub>α</sub>H), 7.3–7.5 (5H, m, aromatic-H). High-resolution FAB mass spectrum consistent with the molecular formula of **1(Et)<sub>2</sub>** (C<sub>21</sub>H<sub>31</sub>N<sub>4</sub>O<sub>8</sub>S). Anal. **1(Et)<sub>2</sub>** (acetate salt) (C<sub>23</sub>H<sub>34</sub>N<sub>4</sub>O<sub>10</sub>S·1.5H<sub>2</sub>O) C: calcd, 6.32; found, 5.83. N: calcd, 9.57; found, 9.42. For **2(Et)<sub>2</sub>** (HCl salt): 300 MHz <sup>1</sup>H NMR (D<sub>2</sub>O, DSS) δ 1.25 (6H, m, ethyl-CH<sub>3</sub>), 2.23 (2H, m, Glu-C<sub>β</sub>H<sub>2</sub>), 2.54 (2H, m, Glu-C<sub>γ</sub>H<sub>2</sub>), 3.21 (1H, q, Cys-C<sub>β</sub>H<sub>a</sub>, *J* = 7.8, 14.5 Hz), 3.42 (1H, q, Cys-C<sub>β</sub>H<sub>b</sub>, *J* = 5.1, 14.5 Hz), 4.02 (2H, s, Gly-CH<sub>2</sub>), 4.15 (4H, m, ethyl-CH<sub>2</sub>), 4.67 (1H, q, Cys-C<sub>α</sub>H, *J* = 5.4, 8.4 Hz), 7.3–7.5 (4H, q, aromatic-H). High-resolution FAB mass spectrum consistent with the molecular formula of **2(Et)<sub>2</sub>** (C<sub>21</sub>H<sub>30</sub>N<sub>4</sub>O<sub>8</sub>SCl). Anal. **2(Et)<sub>2</sub>** (HCl salt) (C<sub>21</sub>H<sub>30</sub>N<sub>4</sub>O<sub>8</sub>SCl<sub>2</sub>·2.5H<sub>2</sub>O) C: calcd, 41.05; found, 40.45. H: calcd, 5.70; found, 5.40. N: calcd, 9.12; found, 9.35. For **3(Et)<sub>2</sub>** (HCl salt): 300 MHz <sup>1</sup>H NMR (D<sub>2</sub>O, DSS) δ 1.25 (6H, m, ethyl-CH<sub>3</sub>), 2.23 (2H, m, Glu-C<sub>β</sub>H<sub>2</sub>), 2.55 (2H, m, Glu-C<sub>γ</sub>H<sub>2</sub>), 2.98 (1H, q, Cys-C<sub>β</sub>H<sub>a</sub>, *J* = 9.8, 14.1 Hz), 3.43 (1H, q, Cys-C<sub>β</sub>H<sub>b</sub>, *J* = 5.1, 14.5 Hz), 4.01 (2H, s, Gly-CH<sub>2</sub>), 4.19 (4H, m, ethyl-CH<sub>2</sub>), 4.67 (1H, q, Cys-C<sub>α</sub>H, *J* = 5.1, 7.65 Hz), 7.5 (4H, q, aromatic-H). High-resolution FAB mass spectrum consistent with the molecular formula of **3(Et)<sub>2</sub>** (C<sub>21</sub>H<sub>30</sub>N<sub>4</sub>O<sub>8</sub>SBr). Anal. **3(Et)<sub>2</sub>** (HCl salt) (C<sub>21</sub>H<sub>30</sub>N<sub>4</sub>O<sub>8</sub>S·2.5H<sub>2</sub>O) C: calcd, 38.27; found, 38.01. H: calcd, 5.32; found, 5.36. N: calcd, 8.51; found, 8.85.

***S*-(*N*-(*p*-Chlorophenyl)-*N*-hydroxycarbamoyl)glutathione [Glycyl] Monoethyl Ester (2[glycyl](Et))**. This compound was prepared by acid-catalyzed esterification of **2** in ethanolic HCl (6 N) (~10 min, room temperature). Removal of the solvent in vacuo gave the hydrochloride salt of the monoethyl ester in 83% yield. This preparation was then purified by reverse-phase C-18 column chromatography using methanol/water (1:1) purified by reverse-phase column chro-



matography as described above. The 300 MHz  $^1\text{H}$  NMR ( $\text{D}_2\text{O}$ , DSS) spectrum of the product was similar to that reported above for  $\mathbf{2}(\text{Et})_2$ , with the exception that the integrated intensities were consistent with a monoethyl ester. The tandem MS/MS spectrum of the product was consistent with a [glycyl] monoethyl ester:  $(\text{M}^{(35}\text{Cl}) + \text{H})^+$ , 505; major fragment ions ( $^{35}\text{Cl}$ ) 402, 376, 130, 104.

**Cell Culture and Cytotoxicity Studies.** Murine lymphocytic leukemia (L1210, G050141) and B16 melanotic melanoma cells were obtained from the NCI, DCT, Tumor Repository (Frederick, MD) and were maintained in RPMI 1640 medium containing L-glutamate (Gibco BRL, Gaithersburg, MD), supplemented with 10% heat-inactivated fetal calf serum and gentamycin (10  $\mu\text{g}/\text{mL}$ ), under 37  $^\circ\text{C}$  humidified air containing 5%  $\text{CO}_2$ . Under these conditions, L1210 and B16 cells have doubling times of approximately 14 and 26 h, respectively. For the cytotoxicity studies, cells in logarithmic growth were introduced into 96-well tissue culture plates at a density of 5000 cells/well (0.15 mL) in the absence and presence of at least five different concentrations of drug, spanning the  $\text{GI}_{50}$  concentration (in triplicate). Aliquots of fresh diethyl ester, from concentrated aqueous stock solutions ( $\sim 10$ – $15$  mM), were added to the media every 12 h, in order to compensate for spontaneous deesterification of the diethyl ester in the growth medium. Aqueous stock solutions of the diethyl esters were stored at  $-80$   $^\circ\text{C}$ . Under these conditions there is no detectable hydrolysis of the diethyl esters over a period of at least 2 weeks. After a 48-h incubation period, the L1210 cells were harvested and washed with fresh media. The B16 cells were washed with Hank's balanced salt solution without  $\text{Ca}^{2+}$  and  $\text{Mg}^{2+}$ , trypsin was added to each well, and the cells were incubated for 10 min at 37  $^\circ\text{C}$ . The trypsin digestion was stopped by the addition of complete media. Cells were centrifuged at 1000g and suspended in fresh media. Cell densities were determined with the use of a Coulter Counter (model ZBI, Coulter Electronics). Cell viability was determined by the trypan blue-exclusion method.<sup>29</sup>

Murine splenic lymphocytes were extruded from freshly excised spleens using RPMI 1640 medium. Cell clumps and connective tissue debris were allowed to settle under gravity, the supernatant fraction was layered onto a Ficoll Hypaque gradient, and the lymphocytes were isolated by centrifugation at 1200g (30 min). (Microscopic examination of the lymphocyte fraction indicated the presence of approximately 10–15 red cells/ $10^6$  lymphocytes.) The lymphocytes were maintained in RPMI 1640 medium, supplemented with 10% heat-inactivated fetal calf serum,  $\beta$ -mercaptoethanol (4  $\mu\text{g}/\text{mL}$ ), nonessential amino acids (Gibco BRL), and gentamycin (10  $\mu\text{g}/\text{mL}$ ), under 37  $^\circ\text{C}$  humidified air containing 5%  $\text{CO}_2$ . For cytotoxicity studies, cells were introduced into 96-well tissue culture plates at an initial density of 120 000 cells/well (0.15 mL) in the absence and presence of different concentrations of drug (in triplicate). Incubation conditions and the determination of the concentration of viable cells were as described above, with the exception that prior to cell counting, the cell suspensions were pretreated with ZAP-OGLOBIN (Coulter Diagnostics), according to the accompanying protocol, in order to reduce the number of contaminating red cells.

**Cell Permeability Studies.** To separate suspensions of L1210 cells ( $1.7 \times 10^6$  cells/mL) in RPMI 1640 medium, containing 10% heat-inactivated fetal calf serum, gentamycin (10  $\mu\text{g}/\text{mL}$ ), and L-glutamate, at 37  $^\circ\text{C}$ , were added compounds  $\mathbf{2}$  and  $\mathbf{2}(\text{Et})_2$  to final concentrations of 0.15 and 0.10 mM, respectively. Aliquots (1 mL) were removed from the cell suspensions as a function of time, and each was overlaid onto 0.4 mL of silicone oil (SF-1250 silicone fluids, General Electric Co., Silicone Products Division, Waterford, NY) contained in an Eppendorf centrifuge tube and centrifuged at 13000g (15 min) at 4  $^\circ\text{C}$ . The supernatant and silicone oil were decanted from the cell pellet, and residual oil was removed from the inside of the centrifuge-tube with a cotton swab. To the pellet was added 1 mL of 70% ethanol in water, and the suspension was sonicated for 5 min. Denatured protein was removed by centrifugation (13000g, 15 min), and the clear supernatant was

brought to dryness under a stream of clean air. The resulting residue was fractionated by reverse-phase HPLC (Waters  $\mu\text{Bondapak C}_{18}$ ,  $0.78 \times 30$  cm), using a mobile phase composed of 45% methanol in water containing 0.25% acetic acid ( $\lambda = 259$  nm):  $\mathbf{2}$ , 17 min;  $\mathbf{2}(\text{Et})_2$ , 26 min;  $\mathbf{2}[\text{glycyl}](\text{Et})_2$ , 30 min. The concentrations of these species were interpolated from standard curves of integrated peak intensity, obtained from reverse-phase fractionation of L1210 cells (as described above), versus the known amounts of  $\mathbf{2}$ ,  $\mathbf{2}(\text{Et})_2$ , or  $\mathbf{2}[\text{glycyl}](\text{Et})_2$  introduced into the cells prior to fractionation. The standard curves were linear in the range 0.02–1.0 nmol ( $r = 0.997$ ). The lower limits of detection of  $\mathbf{2}$  and  $\mathbf{2}(\text{Et})_2$  were empirically determined to be 0.02 nmol, defined as that amount of material giving a signal-to-noise ratio of 3.

**Glyoxalase Activities in L1210 Cells and Splenic Lymphocytes.** Cell pellets, containing approximately  $2 \times 10^7$  L1210 cells or approximately  $7 \times 10^7$  splenic lymphocytes, were lysed in 0.5 mL of ice-cold sodium phosphate buffer (50 mM, pH 7.0) using a Potter-Elvehjem tissue grinder. Cell debris was removed by centrifugation at 13000g (20 min) at 40  $^\circ\text{C}$ . The  $V_{\text{max}}$  units of GlxI and GlxII in the supernatant fractions were obtained on the basis of hyperbolic fits of the initial rate data to the Michaelis–Menten expression. For GlxI, the initial rates of formation of *S*-D-lactoylglutathione versus [GSH-methylglyoxal thiohemiacetal] were followed at 240 nm ( $\Delta\epsilon_{240} = 2860 \text{ M}^{-1} \text{ cm}^{-1}$ ) in sodium phosphate buffer (50 mM, pH 7.0, 25  $^\circ\text{C}$ ), maintaining free GSH at 0.1 mM.<sup>16</sup> For GlxII, the initial rates of loss of *S*-D-lactoylglutathione versus [*S*-D-lactoylglutathione] were followed at 240 nm ( $\epsilon_{240} = 3300 \text{ M}^{-1} \text{ cm}^{-1}$ ) in phosphate buffer (50 mM, pH 7.0, 25  $^\circ\text{C}$ ). The concentrations of protein in the supernatant fractions were determined by the Bradford method, using bovine serum albumin as the reference standard.<sup>30</sup>

**Stability of  $\mathbf{2}(\text{Et})_2$  in Human Serum and Mouse Serum.** To 0.5-mL portions of either human serum or mouse serum, at 37  $^\circ\text{C}$ , was added compound  $\mathbf{2}(\text{Et})_2$  to an initial concentration of approximately 0.15 mM. As a function of time, 0.1-mL aliquots of the incubation mixture were transferred to separate microfuge tubes. The samples were immediately deproteinized by the addition of 70% ethanol (0.9 mL). After incubation for 30 min at 37  $^\circ\text{C}$ , the protein precipitate was sedimented by centrifugation at 13000g. The supernatants were then fractionated by reverse-phase HPLC, as described above, and the integrated intensities of the peaks corresponding to  $\mathbf{2}(\text{Et})_2$  determined. The rate constants for deethylation were calculated from the first-order rate of loss of  $\mathbf{2}(\text{Et})_2$  as a function of time.

**Partition Coefficients.** The *n*-octanol/water partition coefficients for  $\mathbf{2}$  and  $\mathbf{2}(\text{Et})_2$  were obtained by methods analogous to that of Hansch.<sup>31</sup> Compound  $\mathbf{2}$  or  $\mathbf{2}(\text{Et})_2$  was added to a mixture composed of different volumes of phosphate buffer (50 mM, pH 7) (saturated with *n*-octanol) and *n*-octanol (saturated with phosphate buffer (50 mM, pH 7)) to approximately 0.1 mM. The mixture was stirred vigorously at room temperature until equilibrium was achieved ( $\sim 3$  h), as indicated by the constant concentrations of solute species in the organic and aqueous layers (detected either spectrophotometrically or by reverse-phase  $\text{C}_{18}$  column chromatography). The organic and aqueous layers were allowed to separate, and the layers clarified by centrifugation. For  $\mathbf{2}$ , the concentration in the aqueous layer was determined spectrophotometrically ( $\epsilon_{259} = 13 489 \text{ M}^{-1} \text{ cm}^{-1}$ ), and the concentration in the organic layer was determined by difference. For  $\mathbf{2}(\text{Et})_2$ , the organic and aqueous layers were fractionated by reverse-phase  $\text{C}_{18}$  column chromatography and the relative concentrations in the layers determined from the integrated intensities of the peaks corresponding to  $\mathbf{2}(\text{Et})_2$ . Analysis by column chromatography provided a control for partial hydrolysis of  $\mathbf{2}(\text{Et})_2$  in the aqueous layer. For these studies, the partition coefficient ( $p$ ) is defined as the ligand concentration in the organic layer divided by that in the aqueous. Each determination was done in triplicate at different volume ratios of *n*-octanol to phosphate buffer. For compound  $\mathbf{2}$ , the ratios were 5:1 and 50:1; for

compound **2**(Et)<sub>2</sub>, the ratios were 1:1, 1:5 and 1:10. Average values and standard deviations are reported.

**Acknowledgment.** This work was supported by a grant from the National Institutes of Health (CA 59612), a Sigma Xi grant-in-aid of research (to M.J.K.), and a graduate research assistantship from the University of Maryland Baltimore County Designated Research Initiative Fund. M.B.W. was the recipient of the Doris and Merrell Rief Summer Student Fellowship. We are grateful to Elynn Sharkey of this laboratory for preparing **2**[glycyl](Et). We are also grateful to one of the reviewers for suggesting that we test for enhanced sensitivity of L1210 cells to methylglyoxal after exposure of the cells to **2**(Et)<sub>2</sub>.

## References

- Thornalley, P. J. Advances in glyoxalase research. Glyoxalase expression in malignancy, anti-proliferative effects of methylglyoxal, glyoxalase I inhibitor diesters and S-D-lactoylglutathione, and methylglyoxal-modified protein binding and endocytosis by the advanced glycation end product receptor. *Crit. Rev. Oncol. Hematol.* **1994**, *20*, 99–128.
- Creighton, D. J.; Pourmotabbed, T. Glutathione-dependent aldehyde oxidation reactions. In *Molecular Structure and Energetics: Principles of Enzyme Activity*; Liebman, J. F., Greenberg, A., Eds.; VCH Publishers: New York, 1988; Vol. 9, pp 353–386.
- Vander Jagt, D. L. The Glyoxalase system. In *Coenzymes and Cofactors: Glutathione*; Dolphin, D., Poulson, R., Avramovic, O., Eds.; John Wiley and Sons: New York, 1989; Vol. 3 (Part A), pp 597–641.
- Richard, J. P. Kinetic parameters for the elimination reaction catalyzed by triosephosphate isomerase and an estimation of the reaction's physiological significance. *Biochemistry* **1991**, *30*, 4581–4585.
- Reiffen, K. A.; Schneeder, F. A. A comparative study on proliferation, macromolecular synthesis and energy metabolism of *in vitro*-grown Ehrlich ascites tumour cells in the presence of glucosone, galactosone and methylglyoxal. *J. Cancer Res. Clin. Oncol.* **1984**, *107*, 206–210.
- Ayoub, F. M.; Allen, R. E.; Thornalley, P. J. Inhibition of proliferation of human leukaemia 60 cells by methylglyoxal *in vitro*. *Leuk. Res.* **1993**, *17*, 397–401.
- Baskaran, S.; Balasubramanian, K. A. Toxicity of methylglyoxal towards rat enterocytes and colonocytes. *Biochem. Int.* **1990**, *212*, 166–174.
- Ray, M.; Halder, J.; Dutta, S. K.; Ray, S. Inhibition of respiration of tumor cells by methylglyoxal and protection of inhibition by lactaldehyde. *Int. J. Cancer* **1991**, *47*, 603–609.
- White, J. S.; Rees, K. R. Inhibitory effects of methylglyoxal on DNA, RNA and protein synthesis in cultured guinea pig karatocytes. *Chem.-Biol. Interact.* **1982**, *38*, 339–347.
- Papoulis, A.; Al-Abed, Y.; Bucala, R. Identification of N<sup>2</sup>-(1-carboxyethyl)guanine (CEG) as a guanine advanced glycation end product. *Biochemistry* **1995**, *34*, 648–655.
- Ranganathan, S.; Walsh, E. S.; Tew, K. D. Glyoxalase I in detoxification: studies using a glyoxalase I transfectant cell line. *Biochem. J.* **1995**, *309*, 127–131.
- Vince, R.; Daluge, S. A possible approach to anticancer agents. *J. Med. Chem.* **1971**, *14*, 35–37.
- Lo, T. W. C.; Thornalley, P. J. Inhibition of proliferation of human leukaemia 60 cells by diethyl esters of glyoxalase inhibitors *in vitro*. *Biochem. Pharmacol.* **1992**, *44*, 2357–2363.
- Thornalley, P. J.; Ladan, M. J.; Ridgeway, S. J. S.; Kang, Y. Antitumor activity of S-(p-bromobenzyl)glutathione diesters *in vitro*: a structure activity study. *J. Med. Chem.* **1996**, *39*, 3409–3411.
- Thornalley, P. J.; Edwards, L. G.; Kang, Y.; Wyatt, C.; Davies, N.; Ladan, M. J.; Double, J. Antitumor activity of S-p-bromobenzylglutathione cyclopentyl diester *in vitro* and *in vivo*. *Biochem. Pharmacol.* **1996**, *51*, 1365–1372.
- Hamilton, D. S.; Creighton, D. J. Inhibition of glyoxalase I by the enediol mimic S-(N-hydroxy-N-methylcarbamoyl)glutathione: the possible basis of a tumor-selective anticancer strategy. *J. Biol. Chem.* **1992**, *267*, 24933–24936.
- Murthy, N. S. R. K.; Bakeris, T.; Kavarana, M. J.; Hamilton, D. S.; Lan, Y.; Creighton, D. J. S-(N-Aryl-N-hydroxycarbamoyl)-glutathione derivatives are tight-binding inhibitors of glyoxalase I and slow substrates for glyoxalase II. *J. Med. Chem.* **1994**, *37*, 2161–2166.
- Jerzykowski, T.; Winter, R.; Matuszewski, W.; Piskorska, D. A reevaluation of studies on the distribution of glyoxalases in animal and tumor tissues. *Int. J. Biochem.* **1978**, *9*, 853–860.
- Ayoub, F.; Zaman, M.; Thornalley, P. J.; Masters, J. Glyoxalase activities in human tumor cell lines *in vitro*. *Anticancer Res.* **1993**, *13*, 151–156.
- Vince, R.; Daluge, S.; Wadd, W. B. Studies on the inhibition of glyoxalase I by S-substituted glutathiones. *J. Med. Chem.* **1971**, *14*, 402–404.
- Boyd, M. R.; Paull, K. D. Some practical considerations and applications of the National Cancer Institute *in vitro* anticancer drug discovery screen. *Drug Dev. Res.* **1995**, *34*, 91–109.
- Shen, H.; Paul, S.; Breuninger, L. M.; Ciaccio, P. J.; Laing, N. M.; Helt, M.; Tew, K. D.; Kruh, G. D. Cellular and *in vitro* transport of glutathione conjugates by MRP. *Biochemistry* **1996**, *35*, 5719–5725.
- Ishikawa, T.; Ali-Osman, F. Glutathione-associated cis-diamminedichloroplatinum(II) metabolism and ATP-dependent efflux from leukemia cells. *J. Biol. Chem.* **1993**, *268*, 20116–20125.
- Creighton, D. J.; Migliorini, M.; Pourmotabbed, T.; Guha, M. K. Optimization of efficiency in the glyoxalase pathway. *Biochemistry* **1988**, *27*, 7376–7384.
- Shih, M. J.; Edinger, J. W.; Creighton, D. J. Diffusion-dependent kinetic properties of glyoxalase I and estimates of the steady-state concentrations of the glyoxalase-pathway intermediates in glycolyzing erythrocytes. *Eur. J. Biochem.* **1997**, *244*, 852–857.
- Thornalley, P. J.; Tisdale, M. J. Inhibition of human promyelocytic leukaemia HL60 cells by S-D-lactoylglutathione *in vitro*. *Leuk. Res.* **1988**, *12*, 897–904.
- Chyan, M. K.; Elia, A. C.; Principato, G. B.; Giovannini, E.; Rosi, G.; Norton, S. J. Fluorenylmethoxycarbonyl glutathione and diesters: inhibition of mammalian GlxII. *Enzyme Protein* **1995**, *48*, 164–173.
- Soares, E. R. Identification of a new allele of Es-1 segregating in an inbred strain of mice. *Biochem. Genetics* **1979**, *17*, 577–583.
- Kaltenbach, J. P.; Kaltenbach, M. H.; Lyons, W. B. Nigrosin for differentiating live and dead cells. *Exp. Cell Res.* **1958**, *15*, 112–117.
- Bradford, M. A rapid and sensitive method for quantitation of microgram quantities of protein utilizing the principle of protein-dye binding. *Anal. Biochem.* **1976**, *72*, 248–254.
- Fujuta, T.; Iwasa, J.; Hansch, C. A new substituent constant,  $\pi$ , derived from partition coefficients. *J. Am. Chem. Soc.* **1964**, *86*, 5175.

JM9708036